PHARMACOLOGY

Copyright © 2018 The Authors, some rights reserved; exclusive licensee American Association for the Advancement of Science. No claim to original U.S. Government Works

G protein subtype–specific signaling bias in a series of CCR5 chemokine analogs

Emily Lorenzen[1], Emilie Ceraudo[1], Yamina A. Berchiche[1]*, Carlos A. Rico[1], Alexandre Fürstenberg[1,2], Thomas P. Sakmar[1,3†], Thomas Huber[1†]

Chemokines and some chemical analogs of chemokines prevent cellular HIV-1 entry when bound to the HIV-1 coreceptors C-C chemokine receptor 5 (CCR5) or C-X-C chemokine receptor 4 (CXCR4), which are G protein–coupled receptors (GPCRs). The ideal HIV-1 entry blocker targeting the coreceptors would display ligand bias and avoid activating G protein–mediated pathways that lead to inflammation. We compared CCR5-dependent activation of second messenger pathways in a single cell line. We studied two endogenous chemokines [RANTES (also known as CCL5) and MIP-1α (also known as CCL3)] and four chemokine analogs of RANTES (5P12-, 5P14-, 6P4-, and PSC-RANTES). We found that CCR5 signaled through both $G_{i/o}$ and $G_{q/11}$. IP_1 accumulation and Ca^{2+} flux arose from $G_{q/11}$ activation, rather than from Gβγ subunit release after $G_{i/o}$ activation as had been previously proposed. The 6P4- and PSC-RANTES analogs were superagonists for $G_{q/11}$ activation, whereas the 5P12- and 5P14-RANTES analogs displayed a signaling bias for $G_{i/o}$. These results demonstrate that RANTES analogs elicit G protein subtype–specific signaling bias and can cause CCR5 to couple preferentially to $G_{q/11}$ rather than to $G_{i/o}$ signaling pathways. We propose that G protein subtype–specific signaling bias may be a general feature of GPCRs that can couple to more than one G protein family.

INTRODUCTION

G protein–coupled receptors (GPCRs) can transmit extracellular cues from many structurally distinct ligands. GPCRs have been envisioned as on-off switches that become activated through the binding of an agonist ligand, which, in turn, can couple to and activate a single Gα protein class ($G_{i/o}$, $G_{q/11}$, $G_{s/olf}$, or $G_{12/13}$). The G protein is a heterotrimeric protein consisting of a Gα subunit in complex with Gβγ subunits, which initially engages with the active GPCR and then dissociates into constituent Gα and Gβγ components. Depending on the particular G protein and its cellular context, either Gα or Gβγ can mediate downstream effector activity through activation or inhibition of enzymes or channels. The active receptor is desensitized through phosphorylation, which, in turn, mediates β-arrestin recruitment. β-Arrestin can facilitate receptor sequestration or internalization in addition to activating noncanonical signaling systems such as mitogen-activated protein kinase pathways. Canonically, GPCR signaling involves sequential activation of a single type of Gα protein class followed by β-arrestin–dependent activation of noncanonical signal pathways. According to the concept of functional selectivity or ligand bias, signaling intensity can be skewed toward either the G protein pathway or the β-arrestin pathway (*1*, *2*). Biased ligands are potentially desirable therapeutic agents that modulate specific signaling pathways relevant to disease processes (*3*). However, designing biased ligands requires a thorough understanding of receptor pharmacology and the appropriate cell-based assay systems to characterize the properties of drug candidates.

One disease target for biased ligands is HIV-1 infection, an ongoing epidemic with about 2.1 million new cases worldwide in 2015. A strategy to reduce transmission of HIV-1 is to prevent its cellular entry (*4*). C-C chemokine receptor 5 (CCR5) is an obligate coreceptor required for cellular viral entry. Cells lacking CCR5 on their surface are not susceptible to most strains of HIV-1 infection (*5*). Although endogenous chemokine agonists reduce the population of CCR5 on the cell surface by inducing receptor internalization, CCR5 agonists are not used as therapeutic agents for two reasons. First, they cause internalization of only a subset of CCR5, allowing HIV-1 to use receptors remaining on the cell surface for cellular entry (*6*). Second, stimulation of G proteins by activated CCR5 also promotes targeted migration of immune cells, leading to undesirable inflammatory side effects and enhanced HIV-1 infection at the site of inflammation (*7*, *8*). In principle, a biased ligand that causes maximal receptor internalization, in the absence of G protein activation to avoid generating an inflammatory response, would be an ideal HIV-1 cellular entry blocker (*9*).

The desire for a biased, therapeutically viable HIV-1 drug that targets CCR5 has motivated the development of several analogs of regulated on activation, normal T cell expressed and secreted (RANTES) with N-terminal modifications (Fig. 1A): PSC-, 6P4-, 5P12-, and 5P14-RANTES (PSC, 6P4, 5P12, and 5P14 hereafter). These RANTES analogs appear to show pronounced signaling bias. Optimization of AOP-RANTES, the first potent, nonsignaling chemokine analog that blocks HIV-1 entry (*10*), has generated PSC, the first highly potent anti–HIV-1 molecule targeting CCR5 to be developed (*11*). PSC apparently behaves as a pharmacological superagonist because it appears to be more efficacious than RANTES at eliciting the release of intracellular Ca^{2+} stores and is more effective at causing internalization of CCR5 (*9*, *12*). Recombinant RANTES analogs including 6P4, 5P12, and 5P14 have high anti–HIV-1 potency. Like PSC, 6P4 behaves as a strong agonist that induces both Ca^{2+} flux and receptor internalization. In contrast, 5P14 does not cause Ca^{2+} flux signaling but induces receptor internalization, suggestive of an internalization or β-arrestin–biased ligand. Last, 5P12 binds to CCR5 but does not demonstrate apparent Ca^{2+} flux or receptor internalization (*9*).

[1]Laboratory of Chemical Biology and Signal Transduction, The Rockefeller University, 1230 York Ave., New York, NY 10065, USA. [2]Department of Inorganic and Analytical Chemistry, University of Geneva, Quai Ernest-Ansermet 30, 1211 Geneva 4, Switzerland. [3]Department of Neurobiology, Care Sciences and Society, Division for Neurogeriatrics, Center for Alzheimer Research, Karolinska Institutet, 141 57 Huddinge, Sweden.
*Present address: B Cell Molecular Immunology Section, Laboratory of Immunoregulation, National Institute of Allergy and Infectious Diseases, U.S. National Institutes of Health, Bethesda, MD 20892, USA.
†Corresponding author. Email: sakmar@rockefeller.edu (T.P.S.); hubert@rockefeller.edu (T.H.)

Downloaded from http://stke.sciencemag.org/ on June 19, 2021

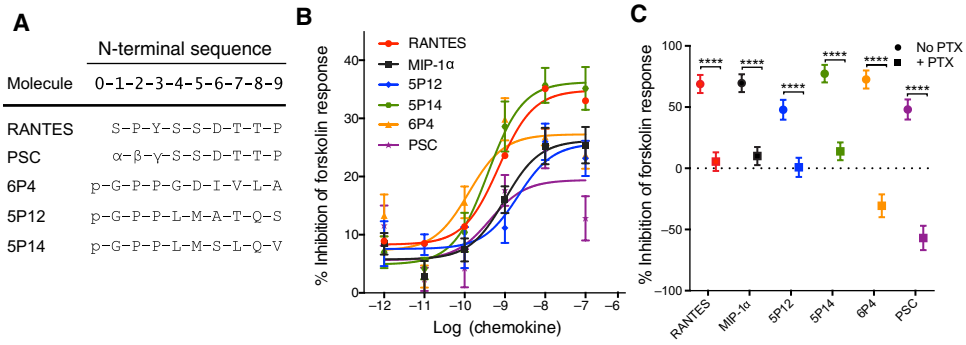

Fig. 1. CCR5-mediated $G_{i/o}$ protein activation by endogenous chemokines and RANTES analogs. (**A**) The RANTES analogs used in this study have modifications to the N-terminal tail region as shown, where p represents pyroglutamate, α represents *N*-nonanoyl, β represents L-thioproline, and γ represents L-2-cyclohexylglycine. (**B**) Human embryonic kidney (HEK) 293T cells cotransfected with CCR5 and the EPAC2 reporter plasmid were stimulated with forskolin and incubated with the chemokines RANTES (red, circle), MIP-1α (black, square), 5P12 (blue, diamond), 5P14 (green, hexagon), 6P4 (yellow, triangle), and PSC (purple, star). (**C**) Transfected cells were pretreated with PTX (100 ng/ml; squares) or control buffer (circles) for 16 hours, stimulated with forskolin, and incubated with 100 nM chemokines. Data are expressed as a percentage of forskolin-stimulated response and are presented as the mean ± SEM for $n \geq 3$ three independent experiments performed in at least technical triplicate. Shown are the statistical significance of the differences between PTX-treated and control condition for each chemokine: ****$P < 0.0001$ (multiple *t* tests). Each chemokine tested significantly inhibited cAMP generation ($P < 0.001$). PSC and 6P4 showed enhanced inhibition of forskolin-induced cAMP generation [$P < 0.05$, one-way analysis of variance (ANOVA), Dunnett's multiple comparisons test].

These RANTES analogs show promise in being capable of tuning the CCR5 signaling pathways to avoid the undesired side effect of inflammation. However, the signaling pathways that link CCR5 activation to its numerous physiological functions, including inflammation, remain poorly characterized. In addition to inducing Ca^{2+} flux, activation of G proteins through CCR5 also leads to inhibition of cyclic adenosine monophosphate (cAMP) generation, an effect of $G_{i/o}$ protein activation. However, it is less clear whether Ca^{2+} flux is a result of G_q protein activation or release of Gβγ subunits after $G_{i/o}$ protein activation in the context of CCR5 (*13*). 5P14, which does not trigger CCR5-mediated Ca^{2+} flux, does inhibit cAMP production (*14*). These results suggest that CCR5-mediated Ca^{2+} flux and inhibition of cAMP generation are not linked and may be mediated by different G proteins. Some GPCRs can signal through more than one Gα protein class depending on the cellular environment and the activating ligand (*15*). CCR5 has been suggested to switch from $G_{i/o}$ to G_q signaling, but the relationship between the well-established $G_{i/o}$ signaling pathway and other G protein signaling pathways remains to be determined (*16*).

Here, we tested the ability of endogenous chemokines and RANTES analogs to activate different Gα protein classes in the same human cell line in culture. It was important to use the same cell line because compositional differences of effectors among cell types can make it possible for a ligand to appear to be biased when different pathways are evaluated in different cells, a bias that is not detected if the same cell types are used for all of the assays (*17*). We measured G protein activation through several downstream pathways, including inhibition of cAMP generation, Ca^{2+} flux, and inositol 1-monophosphate (IP_1) accumulation. In addition, we identified the activated Gα protein subtype that was responsible for these downstream events by performing assays in the presence of transfected individual G proteins or in cells treated with pertussis toxin (PTX) to inactivate $G_{i/o}$ or an inhibitor (YM-254890) to block activation of G_q (*18*, *19*). We found that each of the chemokines induced $G_{i/o}$ protein activation, but the chemokines varied in their ability to activate G_q proteins. In comparison with the endogenous chemokines RANTES (also known as CCL5) and macrophage inflammatory protein-1α (MIP-1α) (also known as CCL3), 6P4 and PSC acted as superagonists at G_q, whereas 5P12 showed no G_q activation and was $G_{i/o}$ biased.

RESULTS

RANTES analogs induce CCR5-mediated inhibition of cAMP production, which depends on $G_{i/o}$ protein activation

We first measured the ability of the RANTES analogs to induce $G_{i/o}$ activation, which is the canonical signaling pathway of CCR5. $G_{i/o}$ activation leads to the inhibition of adenylyl cyclase and a decrease in the amount of cellular cAMP. We tested the ligand-dependent inhibition of forskolin-stimulated cAMP production in cells transfected with CCR5 vector. Each ligand displayed a robust dose-dependent increase in inhibition of cAMP production (Fig. 1B). The EC_{50} (the concentration of ligand required for half-maximal signal) values for inhibition of forskolin-stimulated cAMP accumulation determined for the ligands were all within 20-fold of each other, whereas the E_{max} (maximum signal) values were within about a 2-fold range (Table 1). At the highest concentration of ligand used (100 nM), we found that the range of E_{max} values was 14 to 31% inhibition of the forskolin response. The rank order of maximum signal was 5P14 > RANTES > MIP-1α = 6P4 = 5P12 > PSC. The EC_{50} values of ligands ranged from 0.1 to 2.1 nM with the following rank order: 6P4 > 5P14 > RANTES = PSC > MIP-1α = 5P12 (Table 1). Signaling occurred specifically through CCR5, because empty vector–transfected cells did not show inhibition of cAMP generation in response to any of the chemokines tested (fig. S1). As a control for the effect of changes in CCR5 amount, experiments were also performed 48 hours after transfection (fig. S2), in addition to experiment performed 24 hours after transfection (cf. Fig. 1B).

To confirm that inhibition of cAMP accumulation was due to $G_{i/o}$ protein activation, we measured cAMP accumulation in cells pretreated with PTX to prevent $G_{i/o}$ proteins from interacting with receptors. Similar to the results from the dose-response experiment, each chemokine demonstrated statistically significant CCR5-mediated inhibition of cAMP accumulation in forskolin-treated cells. As expected, PTX pretreatment abrogated the ability of all ligands to inhibit forskolin-stimulated cAMP accumulation (Fig. 1C). 6P4 and PSC also induced significant enhancement of cAMP accumulation above forskolin-stimulated cells after treatment of PTX, as seen as negative percentage values of forskolin inhibition. However, 6P4 and PSC did not induce cAMP accumulation after treatment of PTX when forskolin was not added (fig. S3). We also present raw bioluminescence resonance energy transfer 2 ($BRET^2$) values of the complete time course experiments (fig. S4, A to D).

RANTES analogs have different effects on CCR5-dependent Ca^{2+} flux

In addition to inhibiting cAMP accumulation, CCR5 activation also leads to Ca^{2+} flux. In contrast to inhibiting cAMP accumulation, not

Downloaded from http://stke.sciencemag.org/ on June 19, 2021

Table 1. Summary of fitted curve parameters for inhibition of cAMP accumulation. EC_{50}, pEC_{50}, and E_{max} values with SEM are given for Fig.1B.

	RANTES	MIP-1α	5P12	5P14	6P4	PSC
CCR5						
EC_{50} (nM)	0.7	1	2.1	0.4	0.1	0.4
pEC_{50} ± SEM	−9.2 ± 0.19	−9.0 ± 0.26	−8.7 ± 0.38	−9.4 ± 0.22	−9.9 ± 0.31	−9.4 ± 0.56
E_{max} ± SEM	26 ± 2.3	20 ± 2.5	18 ± 3.2	31 ± 3.1	20 ± 3.0	14 ± 3.4

all of the ligands stimulated Ca^{2+} flux through CCR5 (Fig. 2A). The RANTES analogs induced varying amounts of Ca^{2+} flux with the rank order being 6P4 = PSC > RANTES > MIP-1α > 5P14 > 5P12. Signaling occurred specifically through CCR5, because empty vector–transfected cells did not show Ca^{2+} fluxes in response to any of the chemokines tested (fig. S5). Thus, for Ca^{2+} flux, 6P4 and PSC are superagonists that are more efficacious than the endogenous CCR5 chemokines RANTES and MIP-1α, whereas 5P14 acts as a weak partial agonist and 5P12 does not have agonist activity.

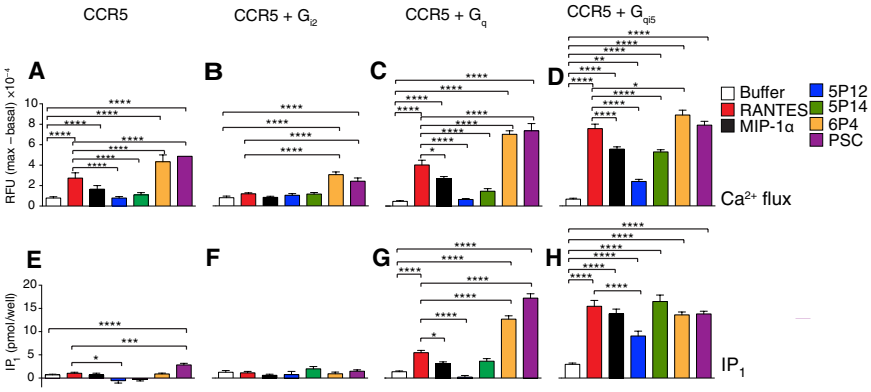

Fig. 2. The effects of G protein–subtype cotransfection on CCR5-mediated Ca^{2+} flux and IP_1 accumulation in response to endogenous chemokines and RANTES analogs. Ca^{2+} flux in HEK293T cells transfected with (**A**) CCR5 alone or with G protein α subunits (**B**) G_{i2}, (**C**) G_q, or (**D**) G_{qi5} was measured in response to 100 nM chemokine. Fluorescence data (maximal minus basal) are presented as mean relative fluorescence units (RFU) ± SEM for $n = 4$ independent experiments performed in technical duplicate. IP_1 accumulation in HEK293T cells transfected with (**E**) CCR5 alone or with G protein α subunits (**F**) G_{i2}, (**G**) G_q, or (**H**) G_{qi5} was measured in response to 100 nM chemokine. Data are expressed as picomoles of IP_1 formed per well and are presented as the mean ± SEM for $n = 4$ independent experiments performed in technical duplicate. Shown are the statistical significance of the differences between chemokine treatment and buffer control and between chemokine treatment and RANTES treatment: $^*P < 0.05$, $^{**}P < 0.01$, $^{***}P < 0.001$, $^{****}P < 0.0001$ (two-way ANOVA, Tukey's multiple comparisons test).

Ca^{2+} flux mediated by CCR5 is inhibited by G_{i2} cotransfection and increased by G_q or G_{qi5} cotransfection

Because of the differences in signaling profiles of the RANTES analogs between Ca^{2+} flux and inhibition of cAMP accumulation, we next investigated the G protein subtype that was responsible for eliciting Ca^{2+} flux through CCR5 activation. Classically, Ca^{2+} flux is a result of G_q protein activation, but chemokine receptors can also induce Ca^{2+} flux through the release of Gβγ subunits after $G_{i/o}$ protein activation (*20*, *21*). To investigate the individual contributions of each G protein subtype to the Ca^{2+} flux signal, we repeated the Ca^{2+} flux experiments in cells in which CCR5 was cotransfected with G_q, G_{i2}, or G_{qi5} protein. G_{qi5} is an engineered G_q protein containing the last five amino acid residues of G_{i2}, which allows $G_{i/o}$-coupled GPCRs to signal through G_q downstream signaling pathways (*22*). Cotransfection of CCR5 with the three G protein subunits did not affect the amount of CCR5 on the cell surface (fig. S6). Also, Ca^{2+} flux in response to adenosine 5′-triphosphate (ATP) in HEK293T cells was not affected by cotransfection of G protein subunits (fig. S7). ATP was used as a positive control to activate endogenous purinergic receptors in HEK293T cells.

Cotransfection of G_{i2} with CCR5 markedly inhibited the ability of RANTES and MIP-1α to induce Ca^{2+} flux through CCR5 (Fig. 2B). G_{i2} cotransfection also dampened the maximum Ca^{2+} flux signal elicited in response to PSC. In contrast, cotransfection of CCR5 and G_q enhanced the maximal Ca^{2+} flux signal for all ligands, except 5P12 (Fig. 2C). In cells cotransfected with CCR5 and a promiscuous G protein construct, G_{qi5}, each RANTES analog induced robust Ca^{2+} flux (Fig. 2D), confirming the ability of all the RANTES analogs to activate $G_{i/o}$ through CCR5. The data were replotted to highlight differences in signal caused by cotransfection of CCR5 with G_q, G_{i2}, or G_{qi5} (fig. S8A).

Because of differences in the binding kinetics of ligands, measurements of ligand bias are sensitive to the experimental time scale (*23*, *24*). For example, Ca^{2+} flux assays measure a transient signal that is complete in 2 min, whereas cAMP accumulation is measured over durations of 15 min or more. To accurately compare the ability of each chemokine to activate CCR5-mediated Ca^{2+} flux and inhibition of cAMP accumulation, it was necessary to measure Ca^{2+} flux with an accumulation assay. Inositol 1,4,5-trisphosphate (IP_3) is a product upstream of Ca^{2+} flux, and a degradation product of IP_3 can be measured by an accumulation assay. Although IP_3 is rapidly degraded, its degradation product IP_1 is stabilized by the addition of lithium chloride, allowing it to accumulate in the cell after receptor stimulation. IP_1 accumulation above that induced by buffer was not seen in vector-transfected negative control cells treated with any ligand (fig. S9). In CCR5-expressing cells, we observed IP_1 accumulation in response to only PSC (Fig. 2E), demonstrating that PSC functions as a superagonist as measured by IP_1 accumulation and Ca^{2+} flux.

Cotransfection of G_{i2} with CCR5 reduced IP_1 accumulation in response to PSC (Fig. 2F). In contrast, G_q cotransfection with CCR5 enhanced IP_1 accumulation in response to each of the chemokines, except 5P12 (Fig. 2G). Moreover, G_q cotransfection with CCR5 revealed agonist activity as measured by IP_1 accumulation in response

Downloaded from http://stke.sciencemag.org/ on June 19, 2021

to 6P4, RANTES, MIP-1α, and 5P14, an effect not seen in cells transfected with only CCR5. In addition, the rank order of maximal IP_1 accumulation signal among the RANTES analogs was similar to that shown for Ca^{2+} flux, with 6P4 = PSC > RANTES > 5P14 > 5P12. Moreover, each of the RANTES analogs showed robust IP_1 accumulation in cells cotransfected with G_{qi5}, confirming that each ligand activates $G_{i/o}$ (Fig. 2H). The data were replotted to highlight differences in signal caused by cotransfection of CCR5 with G_q, G_{i2}, or G_{qi5} (fig. S8B).

Together, our IP_1 accumulation and Ca^{2+} flux data show that PSC and 6P4 are superagonists, whereas 5P12 lacks agonist activity in these assays. Furthermore, G_{i2} cotransfection disrupts the ability of both endogenous CCR5 chemokines and RANTES analogs to induce Ca^{2+} flux and IP_1 accumulation, whereas G_q cotransfection has the opposite effect.

CCR5-mediated Ca^{2+} flux is reduced by inhibiting $G_{i/o}$ protein activation and abolished by inhibiting G_q protein activation

To further differentiate between the contribution of $G_{i/o}$ and G_q proteins to CCR5-mediated signaling, we treated cells with G protein subtype–specific inhibitors. PTX prevents $G_{i/o}$ protein coupling to GPCRs by catalyzing the adenosine 5′-diphosphate ribosylation of a Cys residue in the C-terminal tail of $G_{i/o}$ α subunits (*25*). YM-254890 prevents G_q activation by acting as a guanine-nucleotide dissociation inhibitor of G_q (*26*). Both PTX and YM-254890 decreased CCR5-mediated Ca^{2+} flux (Fig. 3, A to D). However, YM-254890 abolished CCR5-mediated Ca^{2+} flux stimulated by all chemokines, whereas the effects of PTX were less pronounced. In CCR5-expressing cells, PTX reduced Ca^{2+} flux induced by the superagonists 6P4 and PSC and completely inhibited that induced by RANTES and MIP-1α (Fig. 3A). In cells cotransfected with CCR5 and G_{i2}, both PTX and YM-254890 decreased the remaining signal from PSC and 6P4 (Fig. 3B). However, in cells cotransfected with CCR5 and G_q, which would be expected to increase CCR5 signaling, RANTES, MIP-1α, and 5P14 triggered a partially PTX-insensitive Ca^{2+} flux response (Fig. 3C). 6P4 and PSC also showed more PTX insensitivity in cells cotransfected with G_q and CCR5 than in cells expressing CCR5 alone. Last, the signal elicited by chemokines in cells cotransfected with CCR5 and the G_{qi5} chimera was reduced as a result of PTX treatment, except for that triggered by 5P12 (Fig. 3D). Overall, in contrast to PTX, disruption of G_q activation by YM-254890 abolished Ca^{2+} signaling by each ligand even when G_q or G_{qi5} was cotransfected.

CCR5-mediated IP_1 accumulation is reduced by inhibiting $G_{i/o}$ protein activation and abolished by inhibiting G_q

Consistent with the Ca^{2+} flux experiments, YM-254890 prevented all of the chemokines from causing IP_1 accumulation, regardless of the Gα protein subunit cotransfected (Fig. 4, A to D). In cells transfected with CCR5 alone, the PSC-induced IP_1 signal was attenuated by PTX (Fig. 4A). PTX treatment of cells cotransfected with CCR5 and G_q only minimally reduced the IP_1 signal induced by RANTES, MIP-1α, 6P4, and PSC, but had a greater effect on that induced by 5P14 (Fig. 4C). As with Ca^{2+} flux, PTX did not strongly reduce the signal elicited by the RANTES analogs when CCR5 was cotransfected with G_{qi5} (Fig. 4D). In summary, although PTX caused only a modest decrease in chemokine responses, YM-254890 abolished the ability of each of the ligands tested to elicit IP_1 accumulation and Ca^{2+} flux. Thus, both cotransfection and inhibition experiments suggest that G_q is the dominant G protein in stimulating Ca^{2+} flux after CCR5 activation, with $G_{i/o}$ playing a much smaller role.

Cotransfection of CCR5 with $G_{i/o}$, G_q, or G_{qi5} causes different effects on E_{max} values and EC_{50} values

The effects of G protein cotransfection with CCR5 could be a result of a change in ligand E_{max} or EC_{50}. Performing and fitting dose-response curves for Ca^{2+} flux (Table 2) showed that in cells transfected with CCR5, EC_{50} values ranged from 21.0 to 240 nM with the rank order of PSC = 6P4 = RANTES = 5P14 > MIP-1α (Fig. 5A). E_{max} values ranged from 2700 to 45,000 RFU, and the rank order was 6P4 > PSC > RANTES = MIP-1α > 5P14. Similar results were obtained 48 hours after transfection (fig. S10). Cotransfection of CCR5 and G_{i2} decreased Ca^{2+} flux such that only PSC and 6P4 could elicit any Ca^{2+} flux response (Fig. 5B), which was due to reduced E_{max} values because EC_{50} values in cells transfected with CCR5 were similar to those in cells cotransfected with both CCR5 and G_{i2}. Similarly, the increase in response from each chemokine in cells cotransfected with CCR5 and G_q was not a result of altered EC_{50} values, but rather due to an increase in E_{max} values (Fig. 5C). In contrast to G_{i2} and G_q, cotransfection of G_{qi5} and CCR5 altered both EC_{50} and E_{max} values in dose-response Ca^{2+} flux experiments (Fig. 5D). The range of EC_{50} values among the ligands tested decreased, but the rank order was similar, with 6P4 = RANTES > PSC > 5P14 = MIP-1α > 5P12. In addition, the E_{max} value of each ligand increased, but the rank order also remained the same.

In cells transfected with CCR5 alone, only PSC showed any dose-dependent IP_1 accumulation, with an EC_{50} of 190 nM (Fig. 5E) (Table 3). No agonist-stimulated IP_1 accumulation was observed in cells cotransfected with CCR5 and G_{i2} (Fig. 5F). Cells cotransfected with CCR5 and G_q displayed a range of EC_{50} values for IP_1 accumulation of 4.3 to 72 nM with a rank order of 5P14 > 6P4 > RANTES = PSC. These EC_{50} values were similar to those for Ca^{2+} flux (Fig. 5, C and G). The E_{max} values ranged from 1.0 to 8.4 pmol per well with a rank order of PSC > 6P4 > 5P14 > RANTES, although the curve fits for 5P12 and MIP-1α were somewhat ambiguous. This rank order of E_{max} values was similar to that observed with Ca^{2+} flux in CCR5-transfected cells both with and without cotransfection of G_q. As seen previously, cotransfection of G_{qi5} and CCR5 allowed each RANTES analog to cause IP_1 accumulation (Fig. 5H). This increase in signal caused by G_{qi5} cotransfection with CCR5 could be attributed to a decrease in EC_{50} values for all ligands tested. In addition, an increase in E_{max} contributed to the higher signals for RANTES, MIP-1α, 5P12, and 5P14 in cells cotransfected with G_{qi5} and CCR5.

In summary, E_{max} values were altered when $G_{i/o}$ or G_q was cotransfected with CCR5, whereas both E_{max} and EC_{50} values were altered when G_{qi5} was cotransfected with CCR5. These results show that when CCR5 is cotransfected with either G_{i2} or G_q, the E_{max} values, but not the EC_{50} values, for agonist-dependent IP_1 accumulation and Ca^{2+} flux were altered. In contrast, cotransfection of CCR5 and G_{qi5} caused a decrease in EC_{50} values for IP_1 accumulation and Ca^{2+} flux for all ligands tested. In addition, coexpression of CCR5 and G_{qi5} led to an increase in E_{max} values for Ca^{2+} flux for all ligands and an increase in E_{max} values for IP_1 accumulation for most ligands tested.

DISCUSSION

Several GPCR-targeted ligands have been described to cause signaling bias toward β-arrestin or G protein signaling pathways. However,

Downloaded from http://stke.sciencemag.org/ on June 19, 2021

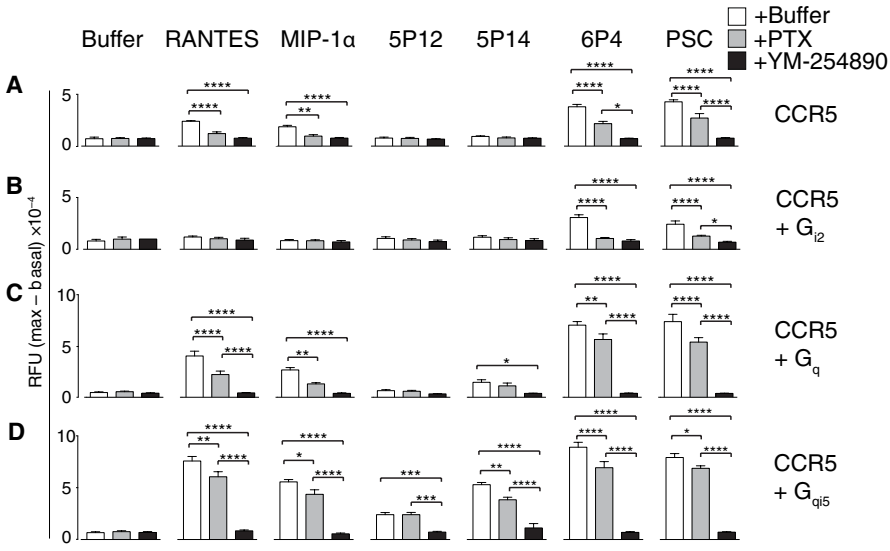

Fig. 3. The effects of PTX and YM-254890 treatment on CCR5-mediated Ca^{2+} flux in response to endogenous chemokines and RANTES analogs. Ca^{2+} flux in HEK293T cells transfected with (**A**) CCR5 alone or with G protein α subunits (**B**) G_{i2}, (**C**) G_q, or (**D**) G_{qi5} was measured in response to 100 nM chemokine. Cells were pretreated with buffer (white bars), PTX (100 ng/ml; gray bars), or 1 μM YM-254890 (black bars). Fluorescence data (maximal minus basal) are presented as mean RFU ± SEM for $n = 4$ independent experiments performed in technical duplicate. Shown are the statistical significance of the differences between buffer control, PTX, and YM-254890: *$P < 0.05$, **$P < 0.01$, ***$P < 0.001$, ****$P < 0.0001$ (two-way ANOVA, Tukey's multiple comparisons test).

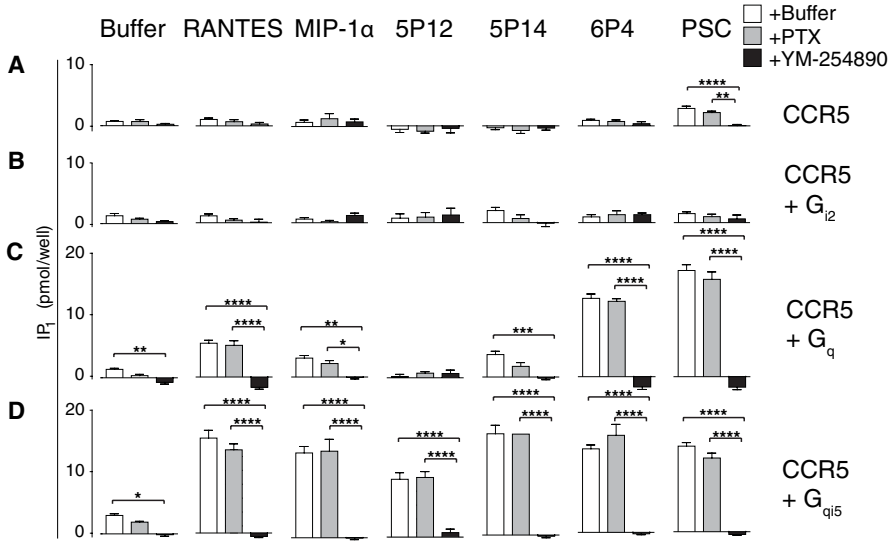

Fig. 4. The effects of PTX and YM-254890 treatment on CCR5-mediated IP_1 accumulation in response to endogenous chemokines and RANTES analogs. IP_1 accumulation in HEK293T cells transfected with (**A**) CCR5 alone or with G protein α subunits (**B**) G_{i2}, (**C**) G_q, or (**D**) G_{qi5} was measured in response to 100 nM chemokine. Cells were pretreated with buffer (white bars), PTX (100 ng/ml; gray bars), or 1 μM YM-254890 (black bars). Data are expressed as picomoles of IP_1 formed per well and are presented as the mean ± SEM for $n = 4$ independent experiments performed in technical duplicate. Shown are the statistical significances of the differences between buffer control, PTX, and YM-254890: *$P < 0.05$, **$P < 0.01$, ***$P < 0.001$, ****$P < 0.0001$ (two-way ANOVA, Tukey's multiple comparisons test).

reports of ligands that bias GPCR signaling toward a specific Gα protein class are rare, in part, because of the difficulty in interpreting signaling assays in which cross-talk between different G protein signaling pathways occurs. In this study, we determined the specific Gα protein class that was responsible for CCR5-mediated inhibition of cAMP accumulation, Ca^{2+} flux, and IP_3 production. Analogs of the endogenous chemokine RANTES with N-terminal modifications showed similar abilities to activate CCR5-mediated $G_{i/o}$ signaling, but either enhanced or decreased abilities to activate CCR5-mediated G_q signaling.

For inhibition of cAMP accumulation, each of the endogenous chemokines and the RANTES analogs tested acted as agonists with similar E_{max} values and EC_{50} values of 2.1 nM or lower. EC_{50} values of at least one order of magnitude higher were obtained earlier from CCR5-expressing Chinese hamster ovary (CHO-CCR5) cells, which also showed a lack of detectable signal for 5P12 (*14*). In addition to the use of different cells, the source of variation between these results could be due to the use of different ligand incubation times or different assays to detect cAMP [real-time changes of cAMP in live cells compared with measurement of cAMP after a single incubation time point (*14*)].

The RANTES analogs showed different abilities to induce Ca^{2+} flux and IP_1 accumulation through CCR5. In comparison to the endogenous chemokines RANTES and MIP-1α, the RANTES analogs 6P4 and PSC acted as superagonists, whereas 5P12 did not have agonist activity in the Ca^{2+} flux assays. Our measurements of EC_{50} and E_{max} values recapitulated the results from Ca^{2+} flux assays performed in CCR5-transfected HeLa-P5L and phytohemagglutinin- and interleukin-2–activated T blasts (*9*). Cells expressing only CCR5 demonstrated IP_1 accumulation in response only to PSC, whereas CCR5-mediated Ca^{2+} flux was measured in response to RANTES, MIP-1α, 6P4, and PSC. The differences between results when assessing Ca^{2+} flux and IP_1 accumulation are likely due to assay sensitivity (*27*). The ability of the RANTES analogs to induce CCR5-mediated G_q signaling appears to correlate with their ability to induce β-arrestin recruitment and internalization. Analogous to the Ca^{2+} flux results, only 5P12 was unable to induce CCR5 internalization (*28*). In addition, cells treated with PSC demonstrated the strongest recruitment of β-arrestin to CCR5, followed by RANTES, and then 5P14. 5P12 did not cause β-arrestin recruitment to CCR5 (*14*, *29*, *30*).

The differences in the signaling profiles of the RANTES analogs suggest that different effectors are responsible for CCR5-mediated inhibition of cAMP accumulation or induction of Ca^{2+} flux. $G_{i/o}$ protein activation inhibits cAMP accumulation, a pathway further confirmed by our results. 6P4 and PSC can stimulate cAMP production above levels induced by forskolin in the presence of PTX, suggesting that these ligands might also stimulate CCR5-mediated G_s protein activation. However, 6P4 and PSC did not demonstrate CCR5-mediated cAMP accumulation in cells treated with PTX, but not with forskolin. The differential regulation of adenylated cyclase

Downloaded from http://stke.sciencemag.org/ on June 19, 2021

Table 2. Summary of fitted curve parameters for Ca^{2+} flux. EC_{50}, pEC_{50}, and E_{max} values with SEM are given for Fig. 5, left column. ND, not detectable.

	RANTES	MIP-1α	5P12	5P14	6P4	PSC
CCR5						
EC_{50} (nM)	32	240	ND	21	36	25
pEC_{50} ± SEM	−7.6 ± 0.2	−6.5 ± 0.2	ND	−7.7 ± 0.7	−7.4 ± 0.1	−7.6 ± 0.1
E_{max} ± SEM	12,000 ± 1000	15,000 ± 2000	ND	3000 ± 1000	45,000 ± 2000	31,000 ± 2000
CCR5 + G_{i2}						
EC_{50} (nM)	ND	ND	ND	ND	110	42
pEC_{50} ± SEM	ND	ND	ND	ND	−6.9 ± 0.3	−7.4 ± 0.3
E_{max} ± SEM	ND	ND	ND	ND	15,000 ± 3000	10,000 ± 2000
CCR5 + G_q						
EC_{50} (nM)	32	460	ND	ND	21	26
pEC_{50} ± SEM	−7.5 ± 0.1	−6.3 ± 0.3	ND	ND	−7.7 ± 0.1	−7.6 ± 0.1
E_{max} ± SEM	20,000 ± 2000	27,000 ± 8000	ND	ND	61,000 ± 4000	64,000 ± 2000
CCR5 + G_{qi5}						
EC_{50} (nM)	0.9	5.1	23	3.6	0.7	1.8
pEC_{50} ± SEM	−9.0 ± 0.1	−8.3 ± 0.1	−7.6 ± 0.1	−8.4 ± 0.1	−9.1 ± 0.1	−8.7 ± 0.1
E_{max} ± SEM	50,000 ± 4000	50,000 ± 3000	19,000 ± 1000	45,000 ± 2000	77,000 ± 4000	67,000 ± 3000

subtypes in HEK293 cells could also be the source of this PTX-dependent cAMP production by 6P4 and PSC. Ca^{2+} can activate certain subtypes of adenylate cyclase, causing cross-talk between Ca^{2+} signaling and cAMP production (*31*). Alternatively, 6P4 and PSC in the presence of PTX could inhibit the degradation of forskolin-dependent cAMP, and these ligands would not induce cAMP production in the presence of PTX, but the absence of forskolin.

The Gα protein subunit that is responsible for Ca^{2+} flux and IP_3 formation is less clear, but could be G_q or $G_{i/o}$. Cotransfection of G_q augments CCR5-mediated Ca^{2+} flux and IP_1 accumulation, responses that are inhibited by cotransfection of G_{i2}, which supports the hypothesis that G_q is responsible for Ca^{2+} flux. G_{i2} transfection could inhibit Ca^{2+} flux and IP_1 accumulation through CCR5 either by preventing G_q recruitment by competitively binding to CCR5 or by acting as a Gβγ subunit scavenger, which would prevent the formation of heterotrimeric G_q proteins required for G protein activity.

We further differentiated the contributions of $G_{i/o}$ and G_q proteins to CCR5-mediated Ca^{2+} flux and IP_3 signaling using inhibitors. The G_q inhibitor YM-254890 prevented all of the RANTES analogs from inducing CCR5-mediated Ca^{2+} flux and IP_1 accumulation. However, the ability of PTX to at least partially inhibit Ca^{2+} flux and IP_1 accumulation does not support the hypothesis that G_q mediates these signaling pathways through CCR5. This seemingly paradoxical result can be explained by the indirect effect of PTX decreasing binding of chemokines to CCR5 (*6*). Reduction of agonist affinity is likely due to a reduction of $G_{i/o}$ protein precoupling to CCR5. Structural studies of β_2 adrenergic receptor interacting with G protein has confirmed the paradigm that a receptor must be bound to a transducer to stabilize the agonist-receptor interaction (*32*). Likewise, the conformation of CCR5 molecules on the cellular surface is altered upon PTX-induced abrogation of $G_{i/o}$ precoupling (*33*). Similar to our results, other reports have also described incomplete inhibition of CCR5-mediated Ca^{2+} flux by PTX, suggesting that $G_{i/o}$ plays a role in agonist binding but not in Ca^{2+} flux (*34*–*36*). Last, it is unlikely that Gβγ subunits could induce Ca^{2+} flux in HEK293T cells, because the closely related HEK293 cell line does not produce the phospholipase C subunit that links Gβγ release to Ca^{2+} flux (*37*). Although we cannot rule out a contribution from Gβγ, our data suggest that Ca^{2+} flux signaling through CCR5 in this cellular system is mainly, if not completely, mediated by G_q protein activation.

Chemokine receptors are historically believed to couple to and signal through $G_{i/o}$ proteins exclusively. The Ca^{2+} flux response elicited by many chemokine receptors has been thought to be a result of Gβγ subunit release after activation of $G_{i/o}$ (*20*). However, we provide evidence that CCR5 signals through both $G_{i/o}$ and $G_{q/11}$ proteins. We also demonstrate that IP_1 accumulation and Ca^{2+} flux are products of G_q protein signaling in HEK293T cells. CCR5 mediates PTX-insensitive signaling responses, suggesting that CCR5 couples to and signals through other G proteins (*16*, *34*, *35*). CCR5 couples to and coimmunoprecipitates with G_q (*38*, *39*). Both G_q and $G_{i/o}$ protein signaling may contribute to the activities of other chemokine receptors. CXCR4 is proposed to switch from $G_{i/o}$ signaling to G_q signaling, leading to reduced migration and activation of the T cells (*16*, *40*). In addition, CXCR4- and CCR7-dependent chemotaxis of dendritic cells requires activation of both $G_{i/o}$ and G_q pathways (*41*). Theoretically, the capacity of a receptor to couple to certain Gα protein subunits should be apparent from its primary structure. However, although residues in similar positions in different GPCRs recognize G proteins, other distinct residues make structural binding contacts. Therefore, without the availability of comparable structures of $G_{i/o}$ and G_q bound to activated GPCRs, it is difficult to surmise whether G_q coupling to other chemokine receptors can be predicted or validated by structural information (*42*).

The capacity of each chemokine to bind to different conformations of CCR5 likely accounts for apparent differences to induce CCR5-mediated signaling in either $G_{i/o}$- or G_q-dependent pathways. The "spare receptor" concept posits that there are at least two pools of inactive CCR5: receptors precoupled to $G_{i/o}$ proteins and "naked"

Downloaded from http://stke.sciencemag.org/ on June 19, 2021

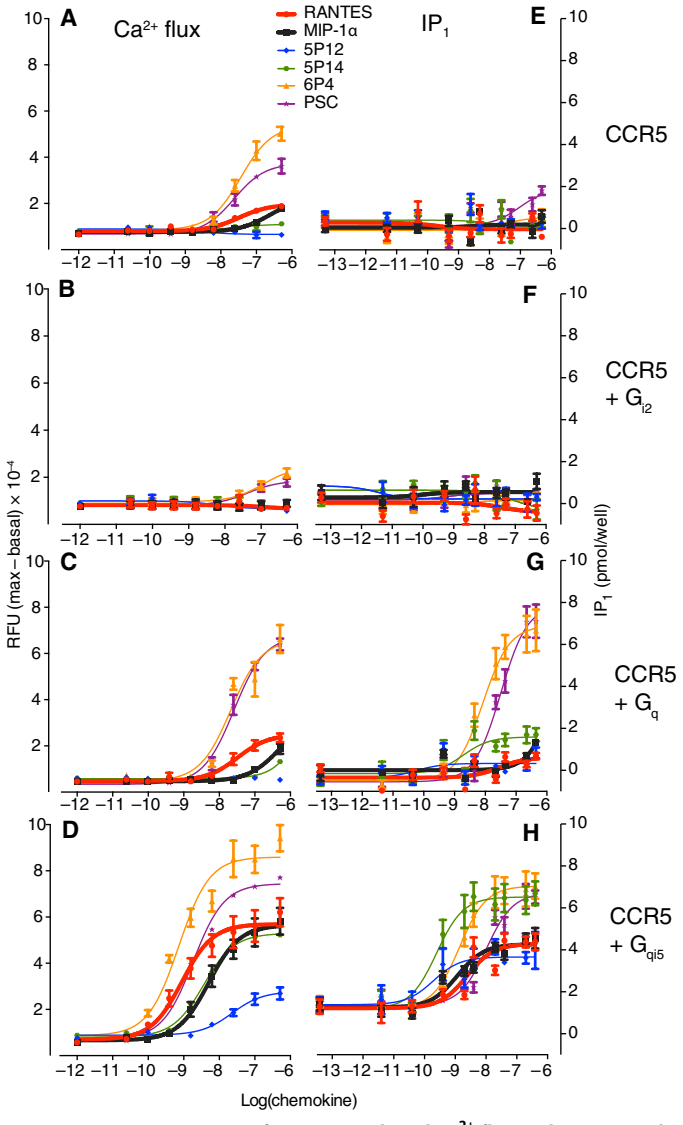

Fig. 5. Dose-response curves for CCR5-mediated Ca^{2+} flux and IP_1 accumulation with or without cotransfection of different G protein α subunits. Ca^{2+} flux in HEK293T cells transfected with (**A**) CCR5 alone or with G protein α subunits (**B**) G_{i2}, (**C**) G_q, or (**D**) G_{qi5} was measured in response to RANTES (red, circle), MIP-1α (black, square), 5P12 (blue, diamond), 5P14 (green, hexagon), 6P4 (yellow, triangle), and PSC (purple, star). Fluorescence data (maximal minus basal) are presented as mean RFU ± SEM for $n = 4$ independent experiments performed in technical triplicate. IP_1 accumulation in HEK293T cells transfected with (**E**) CCR5 alone or with G protein α subunits (**F**) G_{i2}, (**G**) G_q, or (**H**) G_{qi5} was measured in response to RANTES (red, circle), MIP-1α (black, square), 5P12 (blue, diamond), 5P14 (green, hexagon), 6P4 (yellow, triangle), and PSC (purple, star). Data are expressed as picomoles of IP_1 formed per well and are presented as the mean ± SEM for $n = 3$ independent experiments performed in technical triplicate.

receptors not precoupled to $G_{i/o}$ protein (*6*, *43*). CCR5 can assume multiple conformations, as shown by monoclonal antibody detection of different populations of CCR5 (*44*). The endogenous chemokines RANTES and MIP-1α bind with high affinity to only $G_{i/o}$ protein–coupled CCR5, whereas PSC has a high affinity for both $G_{i/o}$ protein–coupled CCR5 and naked CCR5 (*6*). Single-molecule binding experiments have also shown that 5P12, 5P14, PSC, and 6P4 bind to CCR5 with affinities of 374 ± 24 pM, 494 ± 38 pM, 10.1 ± 0.4 pM, and 6.6 ± 0.3 pM, respectively, in detergent solution and in absence of G protein. However, MIP-1α and RANTES do not show detectable binding to naked receptor up to concentrations of 10 μM under these conditions (*45*). Thus, PSC can activate a subset of CCR5 molecules that remains inactive after stimulation with RANTES (*43*). Therefore, the increased Ca^{2+} flux in response to PSC or 6P4 is likely due to the activation of naked CCR5, in addition to $G_{i/o}$ protein–precoupled CCR5. In line with this hypothesis, PSC and 6P4 do not have substantially lower EC_{50} values than RANTES, but do have higher E_{max} values, suggesting that these chemokines are superagonists because they bind to more receptors, rather than because they bind with higher affinity.

We present a model to contextualize the results of our experiments and hypothesize about how RANTES analogs are capable of showing G protein subtype–specific signaling bias (Fig. 6A). For RANTES and MIP-1α, $G_{i/o}$ subunit precoupling promotes binding of the ligand to the receptor, upon which $G_{i/o}$ is activated and dissociates from the receptor. A ligand that remains bound to the receptor can recruit and activate G_q or additional $G_{i/o}$ proteins. In contrast to RANTES and MIP-1α, PSC and 6P4 can bind to and activate CCR5-dependent signaling pathways, independently of whether the receptor is precoupled to $G_{i/o}$ or naked. By signaling through two pools of the receptor, PSC and 6P4 can produce more signals and thus act as superagonists. Although not apparent from our data, 5P12 binds to CCR5 in a G protein–independent fashion (*6*), and thus, binding of 5P12 to naked CCR5 preferentially activates $G_{i/o}$ (Fig. 6B).

This study demonstrates a type of ligand bias that is G protein subtype specific. Another peptide receptor, pituitary adenylate cyclase activating polypeptide (PACAP) receptor, responds to the two ligands PACAP-38 and PACAP-27 with similar EC_{50} values for the G_s signaling pathway. However, the two PACAP receptor ligands have EC_{50} values that are 100-fold different for a G_q signaling pathway (*46*). The free fatty acid receptors (FFARs) also signal through multiple G protein subtypes, but depending on the activating ligand, the FFARs can selectively signal through a single G protein subtype. For example, synthetic agonists targeting FFAR1 can signal through both G_q and G_s, whereas the endogenous agonists signal only through G_q (*47*). In addition, an allosteric modulator targeting FFAR2 selectively activates $G_{i/o}$ signaling but not G_q signaling (*48*). In our study, we described chemokines with similar capacity to evoke CCR5-mediated $G_{i/o}$ signaling, but with both diminished and enhanced G_q signaling.

How the modification of the N-terminal region of RANTES leads to such pronounced changes in CCR5-mediated G_q signaling, but not $G_{i/o}$ signaling, is unclear. Nonetheless, some insight can be garnered from crystal structures of CCR5, including CCR5 in complex with 5P7, another RANTES analog (*49*, *50*). 5P7 differs from 5P12 by one amino acid, Thr instead of Leu at position 7, and lacks agonist activity for Ca^{2+} flux (*9*). When comparing the crystal structure of 5P7 to a model of CCR5 with RANTES, several different interactions are apparent that could be key for G_q protein activation. Whereas RANTES has polar residues in positions 4 to 7 that can engage a minor pocket polar network, 5P7 has bulky hydrophobic residues at these positions. Similarly, the G_q-inactive RANTES analogs 5P12 and 5P14 have bulky hydrophobic residues at positions 4 to 7, whereas the superagonist PSC has polar residues. However, the superagonist 6P4 has mostly less-bulky hydrophobic amino acids at these positions. A crystal structure of CCR5 engaged with a

Downloaded from http://stke.sciencemag.org/ on June 19, 2021

Table 3. Summary of fitted curve parameters for IP_1 accumulation. EC_{50}, pEC_{50}, and E_{max} values are given for Fig. 5, right column. ND, not detectable.

	RANTES	MIP-1α	5P12	5P14	6P4	PSC
CCR5						
EC_{50} (nM)	ND	ND	ND	ND	ND	190
pEC_{50} ± SEM	ND	ND	ND	ND	ND	−6.7 ± 0.4
E_{max} ± SEM	ND	ND	ND	ND	ND	1.7 ± 0.3
CCR5 + G_{i2}						
EC_{50} (nM)	ND	ND	ND	ND	ND	ND
pEC_{50} ± SEM	ND	ND	ND	ND	ND	ND
E_{max} ± SEM	ND	ND	ND	ND	ND	ND
CCR5 + G_q						
EC_{50} (nM)	65	ND	ND	4.3	18	72
pEC_{50} ± SEM	−7.2 ± 0.4	ND	ND	−8.3 ± 0.3	−7.7 ± 0.1	−7.1 ± 0.1
E_{max} ± SEM	1.0 ± 0.2	ND	ND	1.6 ± 0.3	7.4 ± 0.1	8.4 ± 0.1
CCR5 + G_{qi5}						
EC_{50} (nM)	6	2.9	0.5	0.6	3.5	25
pEC_{50} ± SEM	−8.2 ± 0.1	−8.5 ± 0.1	−9.3 ± 0.4	−9.2 ± 0.2	−8.5 ± 0.1	−7.6 ± 0.1
E_{max} ± SEM	3.1 ± 0.3	3.0 ± 0.2	2.3 ± 0.4	5.3 ± 0.4	5.8 ± 0.5	5.4 ± 0.3

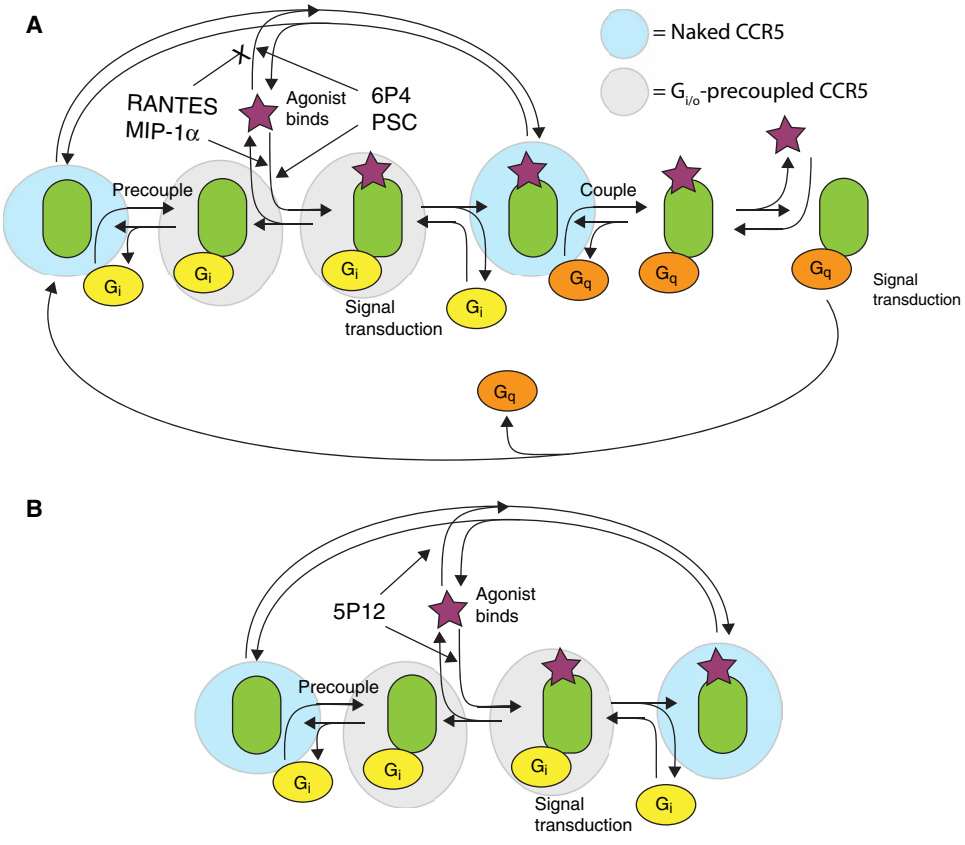

Fig. 6. Conceptual model depicting CCR5-mediated signaling through $G_{i/o}$ and G_q by endogenous chemokines and RANTES analogs. The CCR5 receptor exists in at least two populations, with a group of CCR5 molecules precoupled to $G_{i/o}$ (gray background) and another group in an uncoupled or naked state (blue background). (**A**) RANTES and MIP-1α bind only to $G_{i/o}$-precoupled CCR5, which then leads to activation of $G_{i/o}$. After activation of $G_{i/o}$, CCR5 can then recruit and activate G_q. 6P4 and PSC bind to both $G_{i/o}$-precoupled CCR5 and naked CCR5. Thus, activation of G_q protein occurs independently of $G_{i/o}$ proteins. (**B**) 5P12 binds to both $G_{i/o}$-precoupled CCR5 and naked CCR5, but binding leads to activation of $G_{i/o}$ only.

superagonist will be necessary to understand precisely how G_q signaling is modulated by changes in the N-terminal sequences of RANTES.

The RANTES analogs 5P12 and 5P14, which fail to activate G_q, may be safer drugs because they discriminate between $G_{i/o}$ and G_q protein activation. In bypassing G_q signaling, several physiological effects of CCR5 activation that are PTX resistant or downstream of Ca^{2+} flux would be avoided, including CCR5 recruitment to the immunological synapse during T cell stimulation (*16*). In addition, an in vitro predictor of an inflammatory response, chemotaxis, requires additional GPCR signaling because $G_{i/o}$ signaling is necessary, but not sufficient, to induce chemotaxis (*21*). Because Ca^{2+} flux is necessary for actin rearrangement, an important step in chemotaxis, it is plausible that this additional signaling component is G_q activation (*51*). Although the RANTES chemokine analogs have not been compared in their ability to induce chemotaxis, PSC does cause chemotaxis of CD4 T cells (*6*). The contribution of these two signaling arms to the physiological effects of CCR5 activation remains unknown. Thus, these RANTES analogs could serve as tools to determine the effects of $G_{i/o}$ signaling alone compared with G_q and $G_{i/o}$ protein signaling in combination. Future studies

Downloaded from http://stke.sciencemag.org/ on June 19, 2021

should use these chemokine analogs to determine how CCR5-mediated $G_{i/o}$ and G_q signaling affect events such as chemotaxis and T cell activation using physiologically relevant cell types.

In conclusion, we investigated G protein subtype–specific biased signaling of the chemokine receptor CCR5 using a series of chemokine analogs developed as HIV-1 microbicides. Using a specific inhibitor, we found that $G_{q/11}$ is responsible for Ca^{2+} flux downstream of CCR5 in HEK293T cells, which earlier had been attributed to Gβγ subunit released from $G_{i/o}$. RANTES analogs had a wide range of efficacy for CCR5-mediated G_q signaling, but similar $G_{i/o}$ signaling efficacy, opening the possibility for selectively tuning chemokine signaling. Noncanonical $G_{q/11}$ signaling bias in the chemokine receptor network to our knowledge has not been previously reported. Our findings also provide an experimental strategy in which a G_q-specific inhibitor is used to study G_q signaling bias relevant to Ca^{2+} flux signals from GPCRs thought to couple to $G_{i/o}$.

MATERIALS AND METHODS

Materials

Coelenterazine 400A for $BRET^2$ experiments was from Biotium. The IP-One HTRF assay kit was from Cisbio. Forskolin, PTX, and poly-D-lysine were from Sigma-Aldrich. YM-254890 was from Wako Pure Chemical Industries. Dulbecco's modified Eagle's medium Glutamax (DMEM-Q), Hanks' balanced salt solution (HBSS), and Lipofectamine 2000 were from Life Technologies. Fetal bovine serum (FBS) was from Atlanta Biologicals. Bovine serum albumin (BSA) fraction V, fatty acid free was from Roche, and 96-well white, clear bottom microplates and 384-well black, clear bottom microplates were from Corning. RANTES and MIP-1α were from PeproTech. The RANTES analogs 5P12, 5P14, 6P4, and PSC were a gift from O. Hartley (Université de Genève).

Transfection constructs

The human CCR5 complementary DNA (cDNA) in pcDNA3.1(+) encoded a C-terminal 1D4 epitope tag (TETSQVAPA). The exchange protein directly activated by cAMP 2 (EPAC2) reporter was a gift from M. Bouvier (Université de Montréal). G_q and G_{i2} α subunit plasmids are wild-type human cDNA cloned in pcDNA3.1(+) (cDNA Resource Center). G_{qi5} refers to a construct in which the α subunit of G_q is modified so that its C-terminal tail amino acid residues are derived from the α subunit of G_{i2} (such that EYNLV-COOH in G_q becomes DCGLF-COOH in G_{qi5}). G_{qi5} was cloned into pcDNA1 (Addgene) (*22*).

Cell culture and transfection

HEK293T cells were maintained in DMEM-Q with 10% FBS. Transient transfections were performed using Lipofectamine 2000 according to the manufacturer's instructions with some modifications as previously described (*52*). Cells were transfected in different plate formats with the following amounts of total DNA: 2 μg per well in 6-well plates, 100 ng per well in 96-well plates, and 20 ng per well in 384-well plates. Total transfected plasmid DNA was kept constant by adding empty vector pcDNA3.1(+) when necessary.

Adenylyl cyclase activity assay

Inhibition of forskolin-stimulated cAMP production in response to each chemokine was monitored in HEK293T cells cotransfected with CCR5 and an EPAC reporter protein that shows a decrease in BRET upon cAMP binding (*53*). For each well of a 96-well plate, HEK293T cells (100,000 in 0.1 ml of DMEM) were transfected with 12 ng of RLuc3-EPAC-GFP (green fluorescent protein), a $BRET^2$ cAMP sensor, with or without cotransfection of 24 ng of CCR5 wild type. Cells were then plated at 100 μl per well into 96-well white, clear bottom microplates previously coated with 0.01% (w/v) poly-D-lysine. Twenty-four hours after transfection, medium was replaced with BRET buffer [phosphate-buffered saline (PBS) containing 0.5 mM $MgCl_2$ and 0.1% BSA]. Coelenterazine 400A was added to a final concentration of 5 μM followed by a 5-min incubation at room temperature. Cells were then stimulated with chemokine in the presence or absence of 5 μM forskolin at room temperature for 5 min before $BRET^2$ reading to yield dose-response curves. For kinetic studies, HEK293T cells were transfected as previously described with 15 mM Hepes added to the culture media. Coelenterazine 400A was added in a single column of the 96-well plate, and after 5 min, wells were treated with chemokine in the presence of 5 μM forskolin or 200 μM 3-isobutyl-1-methylxanthine to assess the inhibition of forskolin-stimulated cAMP production or cAMP production, respectively. Then, the plate was immediately read repetitively for 12 min. Cells were treated and wells were read one single column of the 96-well plate at a time, producing one replicate at a time, and repeated six times per plate to produce six replicates per experiment. Luminescence and fluorescence readings were collected using the Synergy NEO2 plate reader (BioTek Instruments) and Gen5 software. $BRET^2$ readings between RLuc3 and GFP10 were collected by sequential integration of the signals detected in the 365- to 435-nm (RLuc3) and 505- to 525-nm (GFP10) windows. $BRET^2$ ratios were calculated as previously described (*52*) and are shown as a percentage of the forskolin-stimulated response. For experiments involving PTX, cells were treated with PTX (100 ng/ml) for 16 hours at 37°C and 5% CO_2 before stimulation with forskolin and chemokines. All experimental manipulations were performed while cells remained attached to the 96-well plates.

Ca^{2+} flux assay

Ca^{2+} mobilization was monitored by loading CCR5-transfected HEK293T cells with a Ca^{2+}-sensitive fluorescent dye and measuring changes in cytosolic Ca^{2+} concentrations immediately after chemokine addition. For each well of a 384-well plate, HEK293T cells (20,000 in 0.02 ml of DMEM) were transfected with 10 ng of CCR5 or 20 ng of empty vector. Where applicable, 5 ng of G_q, G_{i2}, or G_{qi5} vector constructs was cotransfected. Cells were then plated at 20 μl per well into 384-well black, clear bottom microplates previously coated with 0.01% (w/v) poly-D-lysine hydrobromide. Twenty-four hours after transfection, FLIPR Calcium 6 dye (20 μl per well; Molecular Devices) was added to the cells and incubated for 1.5 hours at 37°C with 5% CO_2. The dye was dissolved in HBSS-H [HBSS with 20 mM Hepes (pH 7.4)] with 0.4% BSA. Before measurement, the plate was incubated at 37°C for an additional 30 min in a prewarmed FlexStation II 384 Plate Reader (Molecular Devices). Chemokine at a 5× final concentration was diluted in HBSS-H with 0.2% BSA. Fluorescence readings were collected using the FlexStation plate reader with excitation at 485 nm, emission at 535 nm, and the dichroic mirror at 525 nm. The FlexStation took measurements over a 100-s time course, with 10 μl of ligand added to the cells 20 s after the start of measurement. RFU are reported as the peak magnitude signal minus the basal signal in each well. For experiments involving PTX, cells were treated with PTX (100 ng/ml) for 16 hours at 37°C and 5% CO_2 before chemokine stimulation. For experiments involving

Downloaded from http://stke.sciencemag.org/ on June 19, 2021

YM-254890, 10 μM YM-254890 [dissolved as a 10 mM stock in dimethyl sulfoxide (DMSO)] or equivalent DMSO vehicle was added to the cells and incubated for 30 min at 37°C.

IP_1 accumulation assay

IP_1 concentrations in CCR5-transfected cells were measured using a competitive homogeneous time-resolved fluorescence assay after incubation with each chemokine for 3 hours. For each well of a low-volume, 384-well plate, HEK293T cells (5000 in 7 μl of DMEM) were transfected with 11 ng of CCR5 vector or 11 ng of empty vector. Where applicable, 5.5 ng of G_q, G_{i2}, or G_{qi5} vector constructs was cotransfected. Twenty-four hours after transfection, cells were stimulated by chemokine diluted in 7 μl of 1× stimulation buffer [10 mM Hepes, 1 mM $CaCl_2$, 0.5 mM $MgCl_2$, 4.2 mM KCl, 146 mM NaCl, 5.5 mM glucose, and 50 mM LiCl (pH 7.4)] with 0.2% BSA and 50 mM LiCl (to prevent IP_1 degradation). The chemokine was incubated at 37°C for 3 hours. After incubation, cells were lysed by the addition of d2-fluorophore–labeled IP_1 analog (3 μl per well) as the fluorescence acceptor and the terbium cryptate–labeled anti-IP_1 monoclonal antibody as the fluorescence donor. Both fluorescent donor and acceptor were diluted in the kit-supplied lysis buffer. The plates were incubated overnight at 4°C, and time-resolved fluorescence signals were read using the BioTek Synergy NEO plate reader (BioTek Instruments, Winooski, VT) at 620 and 655 nm. Results were calculated as a 665-nm/620-nm signal ratio, and IP_1 concentrations were interpolated from a standard curve prepared using the supplied IP_1 calibrator. Results are shown as picomoles of IP_1 formed per well. For experiments involving PTX, cells were treated with PTX (100 ng/ml) for 16 hours at 37°C and 5% CO_2 before stimulation. For experiments involving YM-254890, 10 μM YM-254890 or equivalent DMSO vehicle was added to the cells and incubated at 37°C for 30 min.

Measurements of cell surface CCR5

The amount of CCR5 on the cell surface was determined by flow cytometry. For one well of a six-well plate, HEK293T cells (1,000,000 in 2 ml of DMEM) were transfected with 2 μg of empty vector, 1 μg of CCR5 plus 1 μg of empty vector, or 1 μg of CCR5 plus 0.5 μg of G_{i2}, G_q or G_{qi5} and 0.5 μg of empty vector. Twenty-four hours after transfection, cells were detached in ice-cold PBS and transferred to a microcentrifuge tube. Cells were spun down and then incubated with 100 μl of fluorescence-activated cell sorting buffer (PBS with 0.5 mM $MgCl_2$ + 0.1% BSA) containing 8 μl of anti-CCR5 T21/8 phycoerythrin-conjugated antibody (eBioscience) for 60 min on ice. Antibody incubation was followed by three washes with ice-cold PBS. The cell surface receptor amount was quantified by flow cytometry using the Accuri C6 flow cytometer (BD Biosciences) within 1 hour after preparation.

Data analysis

Data were graphed and analyzed using GraphPad Prism 6.0 software (San Diego, CA). Dose-response curves were fitted by a three-parameter logistic equation.

SUPPLEMENTARY MATERIALS

www.sciencesignaling.org/cgi/content/full/11/552/eaao6152/DC1

Fig. S1. Response of cells transfected with EPAC reporter and vector to chemokines and RANTES analogs.

Fig. S2. Dose-response curves for CCR5-mediated $G_{i/o}$ protein activation by chemokines and RANTES analogs using cells expressing higher amounts of CCR5.

Fig. S3. The effect of chemokines and RANTES analogs on cAMP accumulation in the presence of PTX.

Fig. S4. Time courses of CCR5-mediated inhibition of cAMP accumulation induced by chemokines and RANTES analogs.

Fig. S5. Response of vector-transfected cells to chemokines and RANTES analogs through stimulation of Ca^{2+} flux.

Fig. S6. The effect of G protein subunit cotransfection on the amount of CCR5 molecules on the cell surface.

Fig. S7. ATP-induced Ca^{2+} flux in HEK293T cells expressing CCR5 and G protein subunits.

Fig. S8. The effect of G protein subunit cotransfection on CCR5-mediated Ca^{2+} flux and IP_1 accumulation in response to chemokines and RANTES analogs.

Fig. S9. IP_1 accumulation in vector-transfected cells in response to chemokines and RANTES analogs.

Fig. S10. Dose-response curves for CCR5-mediated Ca^{2+} flux in response to chemokines and RANTES analogs using cells expressing higher amounts of CCR5.

REFERENCES AND NOTES

1. L. M. Luttrell, S. Maudsley, L. M. Bohn, Fulfilling the promise of "biased" G protein–coupled receptor agonism. *Mol. Pharmacol.* **88**, 579–588 (2015).
2. J. D. Violin, A. L. Crombie, D. G. Soergel, M. W. Lark, Biased ligands at G-protein-coupled receptors: Promise and progress. *Trends Pharmacol. Sci.* **35**, 308–316 (2014).
3. D. Wacker, R. C. Stevens, B. L. Roth, How ligands illuminate GPCR molecular pharmacology. *Cell* **170**, 414–427 (2017).
4. S. E. Kuhmann, O. Hartley, Targeting chemokine receptors in HIV: A status report. *Annu. Rev. Pharmacol. Toxicol.* **48**, 425–461 (2008).
5. M. Samson, F. Libert, B. J. Doranz, J. Rucker, C. Liesnard, C.-M. Farber, S. Saragosti, C. Lapouméroulie, J. Cognaux, C. Forceille, G. Muyldermans, C. Verhofstede, G. Burtonboy, M. Georges, T. Imai, S. Rana, Y. Yi, R. J. Smyth, R. G. Collman, R. W. Doms, G. Vassart, M. Parmentier, Resistance to HIV-1 infection in Caucasian individuals bearing mutant alleles of the CCR-5 chemokine receptor gene. *Nature* **382**, 722–725 (1996).
6. P. Colin, Y. Bénureau, I. Staropoli, Y. Wang, N. Gonzalez, J. Alcami, O. Hartley, A. Brelot, F. Arenzana-Seisdedos, B. Lagane, HIV-1 exploits CCR5 conformational heterogeneity to escape inhibition by chemokines. *Proc. Natl. Acad. Sci. U.S.A.* **110**, 9475–9480 (2013).
7. P. J. Klasse, R. J. Shattock, J. P. Moore, Which topical microbicides for blocking HIV-1 transmission will work in the real world? *PLOS Med.* **3**, e351 (2006).
8. M. M. Lederman, A. Penn-Nicholson, M. Cho, D. Mosier, Biology of CCR5 and its role in HIV infection and treatment. *JAMA* **296**, 815–826 (2006).
9. H. Gaertner, F. Cerini, J.-M. Escola, G. Kuenzi, A. Melotti, R. Offord, I. Rossitto-Borlat, R. Nedellec, J. Salkowitz, G. Gorochov, D. Mosier, O. Hartley, Highly potent, fully recombinant anti-HIV chemokines: Reengineering a low-cost microbicide. *Proc. Natl. Acad. Sci. U.S.A.* **105**, 17706–17711 (2008).
10. G. Simmons, P. R. Clapham, L. Picard, R. E. Offord, M. M. Rosenkilde, T. W. Schwartz, R. Buser, T. N. C. Wells, A. E. I. Proudfoot, Potent inhibition of HIV-1 infectivity in macrophages and lymphocytes by a novel CCR5 antagonist. *Science* **276**, 276–279 (1997).
11. C. Pastore, G. R. Picchio, F. Galimi, R. Fish, O. Hartley, R. E. Offord, D. E. Mosier, Two mechanisms for human immunodeficiency virus type 1 inhibition by N-terminal modifications of RANTES. *Antimicrob. Agents Chemother.* **47**, 509–517 (2003).
12. O. Hartley, H. Gaertner, J. Wilken, D. Thompson, R. Fish, A. Ramos, C. Pastore, B. Dufour, F. Cerini, A. Melotti, N. Heveker, L. Picard, M. Alizon, D. Mosier, S. Kent, R. Offord, Medicinal chemistry applied to a synthetic protein: Development of highly potent HIV entry inhibitors. *Proc. Natl. Acad. Sci. U.S.A.* **101**, 16460–16465 (2004).
13. C. A. Flanagan, Receptor conformation and constitutive activity in CCR5 chemokine receptor function and HIV infection. *Adv. Pharmacol.* **70**, 215–263 (2014).
14. C. Bönsch, M. Munteanu, I. Rossitto-Borlat, A. Fürstenberg, O. Hartley, Potent anti-HIV chemokine analogs direct post-endocytic sorting of CCR5. *PLOS ONE* **10**, e0125396 (2015).
15. T. Asano, T. Katada, A. G. Gilman, E. M. Ross, Activation of the inhibitory GTP-binding protein of adenylate cyclase, G_i, by β-adrenergic receptors in reconstituted phospholipid vesicles. *J. Biol. Chem.* **259**, 9351–9354 (1984).
16. B. Molon, G. Gri, M. Bettella, C. Gómez-Moutón, A. Lanzavecchia, C. Martínez-A, S. Mañes, A. Viola, T cell costimulation by chemokine receptors. *Nat. Immunol.* **6**, 465–471 (2005).
17. T. Kenakin, Ligand-selective receptor conformations revisited: The promise and the problem. *Trends Pharmacol. Sci.* **24**, 346–354 (2003).
18. J. Takasaki, T. Saito, M. Taniguchi, T. Kawasaki, Y. Moritani, K. Hayashi, M. Kobori, A novel $G\alpha_{q/11}$-selective inhibitor. *J. Biol. Chem.* **279**, 47438–47445 (2004).
19. R. Schrage, A.-L. Schmitz, E. Gaffal, S. Annala, S. Kehraus, D. Wenzel, K. M. Büllesbach, T. Bald, A. Inoue, Y. Shinjo, S. Galandrin, N. Shridhar, M. Hesse, M. Grundmann, N. Merten, T. H. Charpentier, M. Martz, A. J. Butcher, T. Slodczyk, S. Armando, M. Effern, Y. Namkung, L. Jenkins, V. Horn, A. Stößel, H. Dargatz, D. Tietze, D. Imhof, C. Galés, C. Drewke, C. E. Müller, M. Hölzel, G. Milligan, A. B. Tobin, J. Gomeza, H. G. Dohlman, J. Sondek,

Downloaded from http://stke.sciencemag.org/ on June 19, 2021

T. K. Harden, M. Bouvier, S. A. Laporte, J. Aoki, B. K. Fleischmann, K. Mohr, G. M. König, T. Tüting, E. Kostenis, The experimental power of FR900359 to study Gq-regulated biological processes. *Nat. Commun.* **6**, 10156 (2015).
20. M. Thelen, Dancing to the tune of chemokines. *Nat. Immunol.* **2**, 129–134 (2001).
21. E. R. Neptune, H. R. Bourne, Receptors induce chemotaxis by releasing the βγ subunit of G_{i}, not by activating G_q or G_s. *Proc. Natl. Acad. Sci. U.S.A.* **94**, 14489–14494 (1997).
22. B. R. Conklin, Z. Farfel, K. D. Lustig, D. Julius, H. R. Bourne, Substitution of three amino acids switches receptor specificity of $G_q\alpha$ to that of $G_i\alpha$. *Nature* **363**, 274–276 (1993).
23. J. R. Lane, L. T. May, R. G. Parton, P. M. Sexton, A. Christopoulos, A kinetic view of GPCR allostery and biased agonism. *Nat. Chem. Biol.* **13**, 929–937 (2017).
24. C. Klein Herenbrink, D. A. Sykes, P. Donthamsetti, M. Canals, T. Coudrat, J. Shonberg, P. J. Scammells, B. Capuano, P. M. Sexton, S. J. Charlton, J. A. Javitch, A. Christopoulos, J. R. Lane, The role of kinetic context in apparent biased agonism at GPCRs. *Nat. Commun.* **7**, 10842 (2016).
25. D. L. Burns, Subunit structure and enzymic activity of pertussis toxin. *Microbiol. Sci.* **5**, 285–287 (1988).
26. A. Nishimura, K. Kitano, J. Takasaki, M. Taniguchi, N. Mizuno, K. Tago, T. Hakoshima, H. Itoh, Structural basis for the specific inhibition of heterotrimeric G_q protein by a small molecule. *Proc. Natl. Acad. Sci. U.S.A.* **107**, 13666–13671 (2010).
27. K. Liu, S. Titus, N. Southall, P. Zhu, J. Inglese, C. P. Austin, W. Zheng, Comparison on functional assays for Gq-coupled GPCRs by measuring inositol monophospate-1 and intracellular calcium in 1536-well plate format. *Curr. Chem. Genomics* **1**, 70–78 (2008).
28. H. Gaertner, O. Lebeau, I. Borlat, F. Cerini, B. Dufour, G. Kuenzi, A. Melotti, R. J. Fish, R. Offord, J.-Y. Springael, M. Parmentier, O. Hartley, Highly potent HIV inhibition: Engineering a key anti-HIV structure from PSC-RANTES into MIP-1β/CCL4. *Protein Eng. Des. Sel.* **21**, 65–72 (2008).
29. Z. Truan, L. Tarancón Díez, C. Bönsch, S. Malkusch, U. Endesfelder, M. Munteanu, O. Hartley, M. Heilemann, A. Fürstenberg, Quantitative morphological analysis of arrestin2 clustering upon G protein-coupled receptor stimulation by super-resolution microscopy. *J. Struct. Biol.* **184**, 329–334 (2013).
30. L. Tarancón Díez, C. Bönsch, S. Malkusch, Z. Truan, M. Munteanu, M. Heilemann, O. Hartley, U. Endesfelder, A. Fürstenberg, Coordinate-based co-localization-mediated analysis of arrestin clustering upon stimulation of the C–C chemokine receptor 5 with RANTES/CCL5 analogues. *Histochem. Cell Biol.* **142**, 69–77 (2014).
31. J. Hanoune, N. Defer, Regulation and role of adenylyl cyclase isoforms. *Annu. Rev. Pharmacol. Toxicol.* **41**, 145–174 (2001).
32. S. G. F. Rasmussen, B. T. DeVree, Y. Zou, A. C. Kruse, K. Y. Chung, T. S. Kobilka, F. S. Thian, P. S. Chae, E. Pardon, D. Calinski, J. M. Mathiesen, S. T. A. Shah, J. A. Lyons, M. Caffrey, S. H. Gellman, J. Steyaert, G. Skiniotis, W. I. Weis, R. K. Sunahara, B. K. Kobilka, Crystal structure of the β_2 adrenergic receptor-Gs protein complex. *Nature* **477**, 549–555 (2011).
33. A. J. Flegler, G. C. Cianci, T. J. Hope, CCR5 conformations are dynamic and modulated by localization, trafficking and G protein association. *PLOS ONE* **9**, e89056 (2014).
34. M. Farzan, H. Choe, K. A. Martin, Y. Sun, M. Sidelko, C. R. Mackay, N. P. Gerard, J. Sodroski, C. Gerard, HIV-1 entry and macrophage inflammatory protein-1β-mediated signaling are independent functions of the chemokine receptor CCR5. *J. Biol. Chem.* **272**, 6854–6857 (1997).
35. K. Leach, S. J. Charlton, P. G. Strange, Analysis of second messenger pathways stimulated by different chemokines acting at the chemokine receptor CCR5. *Biochem. Pharmacol.* **74**, 881–890 (2007).
36. M. Del Corno, Q.-H. Liu, D. Schols, E. de Clercq, S. Gessani, B. D. Freedman, R. G. Collman, HIV-1 gp120 and chemokine activation of Pyk2 and mitogen-activated protein kinases in primary macrophages mediated by calcium-dependent, pertussis toxin-insensitive chemokine receptor signaling. *Blood* **98**, 2909–2916 (2001).
37. B. K. Atwood, J. Lopez, J. Wager-Miller, K. Mackie, A. Straiker, Expression of G protein-coupled receptors and related proteins in HEK293, AtT20, BV2, and N18 cell lines as revealed by microarray analysis. *BMC Genomics* **12**, 14 (2011).
38. H. Arai, I. F. Charo, Differential regulation of G-protein-mediated signaling by chemokine receptors. *J. Biol. Chem.* **271**, 21814–21819 (1996).
39. A. Mueller, P. G. Strange, CCL3, acting via the chemokine receptor CCR5, leads to independent activation of Janus kinase 2 (JAK2) and G_i proteins. *FEBS Lett.* **570**, 126–132 (2004).
40. J. Ngai, M. Inngjerdingen, T. Berge, K. Taskén, Interplay between the heterotrimeric G-protein subunits $G_{\alpha q}$ and $G_{\alpha i2}$ sets the threshold for chemotaxis and TCR activation. *BMC Immunol.* **10**, 27 (2009).
41. G. Shi, S. Partida-Sánchez, R. S. Misra, M. Tighe, M. T. Borchers, J. J. Lee, M. I. Simon, F. E. Lund, Identification of an alternative $G\alpha_q$-dependent chemokine receptor signal transduction pathway in dendritic cells and granulocytes. *J. Exp. Med.* **204**, 2705–2718 (2007).
42. T. Flock, A. S. Hauser, N. Lund, D. E. Gloriam, S. Balaji, M. M. Babu, Selectivity determinants of GPCR-G-protein binding. *Nature* **545**, 317–322 (2017).
43. J. Jin, P. Colin, I. Staropoli, E. Lima-Fernandes, C. Ferret, A. Demir, S. Rogée, O. Hartley, C. Randriamampita, M. G. H. Scott, S. Marullo, N. Sauvonnet, F. Arenzana-Seisdedos, B. Lagane, A. Brelot, Targeting spare CC chemokine receptor 5 (CCR5) as a principle to inhibit HIV-1 entry. *J. Biol. Chem.* **289**, 19042–19052 (2014).
44. R. Berro, P. J. Klasse, D. Lascano, A. Flegler, K. A. Nagashima, R. W. Sanders, T. P. Sakmar, T. J. Hope, J. P. Moore, Multiple CCR5 conformations on the cell surface are used differentially by human immunodeficiency viruses resistant or sensitive to CCR5 inhibitors. *J. Virol.* **85**, 8227–8240 (2011).
45. C. A. Rico, Single molecule ligand binding studies on CCR5 by fluorescence cross-correlation spectroscopy, Rockefeller University (2017).
46. D. Spengler, C. Waeber, C. Pantaloni, F. Holsboer, J. Bockaert, P. H. Seeburg, L. Journot, Differential signal transduction by five splice variants of the PACAP receptor. *Nature* **365**, 170–175 (1993).
47. M. Hauge, M. A. Vestmar, A. S. Husted, J. P. Ekberg, M. J. Wright, J. Di Salvo, A. B. Weinglass, M. S. Engelstoft, A. N. Madsen, M. Lückmann, M. W. Miller, M. E. Trujillo, T. M. Frimurer, B. Holst, A. D. Howard, T. W. Schwartz, GPR40 (FFAR1)—Combined Gs and Gq signaling in vitro is associated with robust incretin secretagogue action ex vivo and in vivo. *Mol. Metab.* **4**, 3–14 (2015).
48. D. Bolognini, C. E. Moss, K. Nilsson, A. U. Petersson, I. Donnelly, E. Sergeev, G. M. König, E. Kostenis, M. Kurowska-Stolarska, A. Miller, N. Dekker, A. B. Tobin, G. Milligan, A novel allosteric activator of free fatty acid 2 receptor displays unique G_i-functional bias. *J. Biol. Chem.* **291**, 18915–18931 (2016).
49. Y. Zheng, G. W. Han, R. Abagyan, B. Wu, R. C. Stevens, V. Cherezov, I. Kufareva, T. M. Handel, Structure of CC chemokine receptor 5 with a potent chemokine antagonist reveals mechanisms of chemokine recognition and molecular mimicry by HIV. *Immunity* **46**, 1005–1017.e5 (2017).
50. Q. Tan, Y. Zhu, J. Li, Z. Chen, G. W. Han, I. Kufareva, T. Li, L. Ma, G. Fenalti, J. Li, W. Zhang, X. Xie, H. Yang, H. Jiang, V. Cherezov, H. Liu, R. C. Stevens, Q. Zhao, B. Wu, Structure of the CCR5 chemokine receptor-HIV entry inhibitor maraviroc complex. *Science* **341**, 1387–1390 (2013).
51. N. Joseph, B. Reicher, M. Barda-Saad, The calcium feedback loop and T cell activation: How cytoskeleton networks control intracellular calcium flux. *Biochim. Biophys. Acta* **1838**, 557–568 (2014).
52. Y. A. Berchiche, T. P. Sakmar, CXC chemokine receptor 3 alternative splice variants selectively activate different signaling pathways. *Mol. Pharmacol.* **90**, 483–495 (2016).
53. M. Leduc, B. Breton, C. Galés, C. Le Gouill, M. Bouvier, S. Chemtob, N. Heveker, Functional selectivity of natural and synthetic prostaglandin EP_4 receptor ligands. *J. Pharmacol. Exp. Ther.* **331**, 297–307 (2009).

Acknowledgments: We thank M. Bouvier (Université de Montréal) for providing the EPAC reporter cAMP reporter plasmid, B. Conklin (University of California, San Francisco) for the gift of the G_{qi5} transfection vector, and O. Hartley (Université de Genève) for the gift of 5P12, 5P14, 6P4, and PSC. We thank R. Vaughn for help with statistical analysis and M. Kazmi and O. Hartley for critical reading of the manuscript. **Funding:** E.L. was funded by the David Rockefeller Fellowship. E.C. was funded by the François Wallace Monahan Fellowship. We also acknowledge grant support from the Robertson Foundation, the Crowley Family Fund, and the Danica Foundation to T.H. **Author contributions:** E.L., Y.A.B., E.C., C.A.R., A.F., T.H., and T.P.S. designed the experiments. E.L., Y.A.B., E.C., and C.A.R. performed analyses. E.L., T.H., and T.P.S. wrote the paper. **Competing interests:** The authors declare that they have no competing interests. **Data and materials availability:** All data needed to evaluate the conclusions in the paper are present in the paper or the Supplementary Materials.

Submitted 14 September 2017
Accepted 25 September 2018
Published 16 October 2018
10.1126/scisignal.aao6152

Citation: E. Lorenzen, E. Ceraudo, Y. A. Berchiche, C. A. Rico, A. Fürstenberg, T. P. Sakmar, T. Huber, G protein subtype–specific signaling bias in a series of CCR5 chemokine analogs. *Sci. Signal.* **11**, eaao6152 (2018).

Downloaded from http://stke.sciencemag.org/ on June 19, 2021

Science Signaling

G protein subtype–specific signaling bias in a series of CCR5 chemokine analogs

Emily Lorenzen, Emilie Ceraudo, Yamina A. Berchiche, Carlos A. Rico, Alexandre Fürstenberg, Thomas P. Sakmar and Thomas Huber

Sci. Signal. **11** (552), eaao6152.
DOI: 10.1126/scisignal.aao6152

Biasing CCR5 against inflammation

The G protein–coupled chemokine receptor CCR5 is required for the cellular entry of HIV-1. The ideal drug targeting CCR5 to block HIV-1 infection would induce receptor internalization without triggering the undesirable effect of inflammation. Thus, Lorenzen *et al.* characterized the signaling properties of two endogenous ligands of CCR5, RANTES and MIP-1 α, and several RANTES analogs in cells expressing CCR5 with $G_{i/o}$ or $G_{q/11}$ subunits. They found that CCR5 inhibited generation of the second messenger cAMP by stimulating $G_{i/o}$ and induced Ca^{2+} signaling through $G_{q/11}$ and that the RANTES analogs differentially activated $G_{i/o}$ and $G_{q/11}$. The authors hypothesize that RANTES analogs that preferentially stimulate $G_{i/o}$ may block HIV-1 infection without inducing inflammation.

ARTICLE TOOLS http://stke.sciencemag.org/content/11/552/eaao6152

SUPPLEMENTARY MATERIALS http://stke.sciencemag.org/content/suppl/2018/10/12/11.552.eaao6152.DC1

RELATED CONTENT
http://stke.sciencemag.org/content/sigtrans/11/552/eaat2214.full
http://stke.sciencemag.org/content/sigtrans/11/555/eaaq1075.full
http://stke.sciencemag.org/content/sigtrans/11/559/eaat1631.full
http://stke.sciencemag.org/content/sigtrans/12/597/eaat4128.full
http://stke.sciencemag.org/content/sigtrans/13/617/eaaw5885.full

REFERENCES This article cites 52 articles, 20 of which you can access for free
http://stke.sciencemag.org/content/11/552/eaao6152#BIBL

PERMISSIONS http://www.sciencemag.org/help/reprints-and-permissions

Use of this article is subject to the Terms of Service

Science Signaling (ISSN 1937-9145) is published by the American Association for the Advancement of Science, 1200 New York Avenue NW, Washington, DC 20005. The title *Science Signaling* is a registered trademark of AAAS.

Copyright © 2018 The Authors, some rights reserved; exclusive licensee American Association for the Advancement of Science. No claim to original U.S. Government Works

Downloaded from http://stke.sciencemag.org/ on June 19, 2021